CATS: a new autonomous station for atmospheric turbulence characterization

Aziz Ziad[a], Julien Chabé[b], Yan Fantei-Caujolle[a], Eric Aristidi[a], Catherine Renaud[a], and Christophe Giordano[a]

[a]Université Côte d'Azur, OCA, CNRS, Lagrange, Parc Valrose 06108 Nice Cedex 2, France
[b]Université Côte d'Azur, OCA, CNRS, IRD, Géoazur, 2130 route de l'Observatoire, 06460 Caussols, France

ABSTRACT

The Lagrange Laboratory of the University/Observatory of Côte d'Azur has developed recently a new-generation of autonomous instruments within original techniques for measuring optical turbulence since the first meters above the ground to the borders of the atmosphere including the dome seeing. These instruments are part of the Calern Atmospheric Turbulence Station (CATS) developed in the framework of a scientific programme for a better understanding and modeling of optical turbulence for astronomical observations and laser communications. For the first time, the study of the evolution the turbulence profile continuously during the daytime and nighttime is now possible thanks to the PML (Profiler of Moon Limb) instrument. Indeed, the PML measures the C_N^2 and outer scale profiles each 3 minutes using lunar and solar limbs with a resolution reaching 100m in the ground layer. The wavefront parameters at ground level (seeing, outer scale, coherence time and isoplanatic angle) are provided by the Generalized DIMM (GDIMM). The INTENSE (INdoor TurbulENce SEnsor) instrument is occasionally associated with CATS station to measure the turbulence in the dome of the 1.5m MeO telescope and to evaluate its contribution on the observations. The CATS station is also a support for another programme on the prediction of the turbulence. Data provided by CATS are used to constraint the modeling to optimize the prediction.

Keywords: Site-testing, atmospheric optics, atmospheric turbulence,turbulence monitoring.

1. INTRODUCTION

The Calern Observatory of the Observatoire de la Côte d'Azur has been equipped recently with a new generation station for atmospheric turbulence characterization. The Calern Atmospheric Turbulence Station (CATS)[1–3] is the result of a long expertise recognized internationally in Atmospheric Optics. This Lagrange Laboratory's expertise is at the origin of its important role in the selection of the major sites hosting the existing large telescopes in particular of the $8-10$ meter class: GranTeCan in the Canary Islands, the European VLT and Southern Gemini in Chile, Keck, Northern Gemini & Subaru in Hawaii. With a unique set of instruments to probe the atmospheric turbulence, the Lagrange Laboratory was involved in the site selection of the future Extremely Large Telescopes (ELT) as the 40m European E-ELT and the 30m American TMT. Our team was also in charge of the qualification of the site of Dome C in Antarctica whose potential in Astronomy is considerable. In the continuity of this long tradition, the CATS station benefits of a new generation of autonomous instruments within original techniques for measuring optical turbulence since the first meters above the ground to the borders of the atmosphere. One of these instruments is the PML[4] (Profiler of Moon Limb) measuring the vertical distribution of turbulence using lunar and solar edges. The second instrument, called G-DIMM for Generalized DIMM,[5,6] is dedicated to provide wavefront parameters at ground level (seeing, outer scale, coherence time and isoplanatic angle). The third instrument is INTENSE[7,8] (INdoor TurbulENce SEnsor) dedicated to the characterization of optical turbulence inside a dome which can have a significant contribution to the degradation of the optical resolution of the telescope. The CATS station is installed near the MeO telescope at Calern Observatory in the

Further author information: (Send correspondence to A. Z.): E-mail: ziad@unice.fr, Telephone: (33) (0)4 92 07 63 38

South-East of France. This station is a support of other projects at the Calern Observatory, mainly to improve the link budget of Laser Telemetry from MeO station and generally free space optical links. It is also supporting projects on MeO and C2PU telescopes to test and validate new concepts and components in order to overcome the current limitations of existing Adaptive Optics (AO) systems. The idea is to offer to AO community a fully operational on-sky test platform. The ultimate goal being the optimization of the scientific returns of the AO assisted instrumentations.

The CATS station is installed at the Calern Observatory which was inaugurated in 1974 as a laboratory intended for the development and testing of new instruments. The essential qualities of this 20 km^2 semidesertic calcareous plateau are a high number of clear nights, an absence of mists and dusts, a not too dry atmosphere, and a circulation of winds in horizontal layers due to the topography and to the presence of the marine wind which stabilizes the atmosphere. From the 70's to the 90's, the Calern Observatory was the place of birth of many precursory instruments in their discipline, in particular in laser telemetry and interferometry with two telescopes (I2T) and its successor GI2T. The activity of the Schmidt telescope with the large field imaging of small objects was also very intense up to the early 2000s. Currently, the scientific activities of the Calern plateau is centered around projects in the link between astronomy and geophysics such as Satellite Laser Ranging, Lunar Laser Ranging, Time Transfert by Laser Link with the T2L2 space mission, Spatial Geodesy, Measure of the Solar diameter with PICARD-SOL, follow on project of fast transitory objects (TAROT), asteroids photometry and polarimetry (CAPS), double star characterization (PISCO), giant planet sismology (DSI), follow-up of GAIA space telescope alerts. Several projects with industrial partners like Airbus Defence and Space (Geotracker), Thales Alenia Space, or ONERA on adaptive optics are carried on. Recently, the Calern plateau host teaching and training activities for master students through an infrastructure devoted to the immersion of students in the experimental environment in astrophysics and geophysics, the Center for Pedagogy in Planet and Universe sciences (C2PU). All these activities requires a permanent and reliable monitoring of the turbulence conditions above the plateau of Calern, now done by the CATS instruments.

The CATS station is also a support for our training activities as part of our Masters MAUCA and OPTICS, through the organization of on-sky practical works. We are also considering the organization of international summer schools and workshops on the techniques of Atmospheric Optics and Site-Testing in Astronomy around the CATS station.

2. THE CALERN ATMOSPHERIC TURBULENCE STATION: CATS

The CATS station is composed with a set of two autonomous and complementary instruments. The first one is the Generalized Differential Image Motion Monitor (GDIMM),[6] aiming at monitoring all the integrated parameters of the optical turbulence (seeing, isoplanatic angle, coherence time and outer scale). In order to avoid the turbulent surface layer, the GDIMM is installed on a 4 meters high concrete pilar (left of Fig.1). The instrument is protected by a 7ft allsky dome attached to a metallic tower. This tower also supports all the peripheral components of the GDIMM instruments (power management, electronics and computer). To minimize vibrations, the pilar foundation is isolated from the tower foundation. A particular attention was given to the stability of the ground below the instrument as the plateau is characterized by several karstic cavity (sinkholes and dolines). An electric tomography of the ground at the desired position of the station was done to locate possible defects in the underground.

The second instrument is the "Profiler of Moon Limb"[4] which is devoted to the extraction of the $C_n^2(h)$ profile with high vertical resolution using the Moon or Solar limb fluctuations. This instrument is also protected by a 12 ft allsky dome attached to a concrete platform (right of Fig.1). Finally, to make the CATS station works in an autonomous manner, an AllSky camera to monitor the presence of clouds in the sky and a weather station are connected to a set of small computers (Banana Pi) where devoted software runs to give real time information to both instruments for observation management.

2.1 GDIMM instrument

The DIMM is a seeing monitor which is very popular because of its simplicity. It is based on a small telescope with an entrance pupil made of 2 small subapertures, observing a bright single star with a short exposure (typically a few miliseconds). The GDIMM monitor is a compact instrument aiming at replacing the aging Generalized

Figure 1. The CATS station installed near the MeO telescope at Calern Observatory.

Seeing Monitor (GSM).[9,10] GDIMM is very similar to a DIMM,[11] with 3 sub-apertures instead of 2. It has been developed using the experience on the GSM instrument[9] and of the qualification of the Dome C site in Antartica.[12]

The GDIMM instrument is composed by a Schmidt-Cassegrain Celestron 11 telescope (diameter 280 mm) equipped with an entrance mask with 3 sub-pupils as shown in Fig. 2. It is derived from the classical 2-apertures DIMM mask, with a supplementary sub-pupil used for estimating the isoplanatic angle and the outer scale. The two main sub-pupils are circular with a diameter of 6 cm, they are both equipped with a glass prism with a deviation angle of about 30 arcsec. The prisms are oriented to give opposite tilts to the incident light. The mask is oriented so that the aperture separation is parallel to the declination axis. The third sub-aperture is also circular, with a 10 cm diameter and a 4 cm central obstruction. This aperture is left open and the corresponding image is formed on the optical axis. The telescope is placed on an Astro-Physics 900 equatorial mount remotely controlled by a computer via a RS-232 link. In the focal plane, a Prosilica EC650 camera captures the three star image at a maximum frame rate of 90 fps at full resolution (windowing and binning options are available to increase the frame rate if necessary). A Barlow lens increases the focal length to 6.35 meters to allow a slight oversampling of the Airy discs (5 pixels at a wavelength of 500 nm in the Airy disc of the 10 cm diameter sub-pupil). This "science" camera is connected to the computer via an Ethernet cable. Finally, a second camera (USB webcam Logitech 9000) is placed at the focus of a Celestron Travelscope 90, used as a finder with a wide field of 4 degrees. This camera is sensitive enough to detect all the bright stars (Mag < 2) used for the GDIMM monitoring of the turbulence.

The images given by the science camera are treated by a dedicated acquisition software written in C++/QT which takes benefit of years of developments of automated instruments for the Antarctic. It can point the mount to the desired star, detects and centers automatically the target on the finder and on the science camera. Observations can be made manually or by acquisition sequences. Seeing, isoplanatic angle, coherence time and outer scale are computed in real time. Various tests are performed to stop the observations when the star is lost (clouds) or if its zenithal distance becomes too large (Star target change). Data are written in text-based csv files but it is also possible to record the images in FITS cubes. Each measurement is finally sent to a website available for the users of the observatory and the general public (see Fig.7).

The most important parameter provided by the GDIMM instrument is the seeing (or Fried parameter) and

Figure 2. The GDIMM instrument inside its 7 ft AllSky dome which is installed on a platform at $4m$ above ground level (left of Fig.1).

that's why usually this kind of instruments is called seeing monitor. The seeing is extracted from Angle-of-Arrival (AA) fluctuations of the perturbed wavefronts. These AA fluctuations are obtained through the two GDIMM $6cm$ apertures from twin images tilts in the focal plane. Angular distances α and β (called Angle-of-Arrival) of the centroid of each star image are computed in both directions (α is parallel to the basis of the sub-apertures). Longitudinal and transversal differential variances (σ_l^2 and σ_t^2 respectively) of α and β are estimated on a sequence of N instantaneous snapshots (N being typically several hundreds). From these differential variances, the seeing ϵ (in radian) is deduced using the following formulae:

$$\epsilon_{l|t} = 0.98\,(\cos z)^{-0.6}\,\left(\frac{D}{\lambda}\right)^{0.2}\,\left(\frac{\sigma_{l|t}^2}{K_{l|t}}\right)^{0.6} \tag{1}$$

where $K_l = 0.364\,(1 - 0.532b^{-1/3} - 0.024b^{-7/3})$ and $K_t = 0.364\,(1 - 0.798b^{-1/3} + 0.018b^{-7/3})$, B is the distance between the sub-apertures, D their diameter, $b = B/D$, z is the zenithal distance and λ the wavelength, traditionally set to 500 nm as a standard. Two estimations of the seeing are obtained for a given sequence, they are supposed to be the almost identical (isotropic hypothesis) if the exposure time is short enough in regards to the turbulence coherence time. The seeing and the Fried parameter r_0 ($\epsilon = 0.98\,\frac{\lambda}{r_0}$) are wavelength λ depending varying as $\lambda^{-1/6}$ and $\lambda^{6/5}$, respectively.

Another important parameter characterizing the wavefronts perturbed by the turbulence, is the isoplanatic angle θ_0. This latter can be estimated from the scintillation of a single star observed through a pupil of diameter $10cm$ and a central obstruction of $4cm$. The principle of this θ_0 estimation method is based on the similarity of the theoretical expressions of θ_0 and the scintillation index s.[9,13] θ_0 is obtained in arcsec for a wavelength $\lambda = 500nm$ by the following formula using the third sub-aperture of GDIMM (Fig. 2):

$$\theta_0^{-5/3} = A\,(\cos z)^{-8/3}\,s \tag{2}$$

where $A = 14.87$[9] and z is the zenithal angle of the observed star.

The most difficult parameter to measure is the wavefront coherence outer scale $\mathcal{L}_0$.[14] In the case of the GDIMM instrument, we propose to use variances of AA fluctuations through different size sub-apertures by means of the von Karman model. The AA variance of the image of a star observed through a small aperture of diameter D is given, in square radians by:[15] $\sigma_D^2 = 0.17\,\lambda^2\,r_0^{-5/3}\,[D^{-1/3} - 1.525\mathcal{L}_0^{-1/3}]$. For isotropic turbulence, the variances in x and y directions are identical. The pupil of GDIMM has 3 apertures, two of diameter $D_1 = D_2 = 6$ cm, one of diameter $D_3 = 10$ cm. A normalized AA variance by variance difference or by

differential variance is used in the GDIMM to provide estimations of the outer scale $\mathcal{L}_0$.[5,6,16] Since the GDIMM has two $6cm$ subapertures, one can deduce different estimations of $\mathcal{L}_0$.

In the other hand, the coherence time τ_0 relevant for adaptive optics and interferometry, is given by:[17] $\tau_0 = 0.31\,\frac{r_0}{\bar{v}}$, where $\bar{v}$ the effective wind speed, is a weighted average of the wind speed on the whole atmosphere.[17] We had shown[10] that it is possible to derive the effective wind speed from the temporal structure functions $D_{\alpha|\beta}(\tau)$ of the AA fluctuations, defined as $D_{\alpha|\beta}(\tau) = \langle[\alpha|\beta(t) - \alpha|\beta(t+\tau)]^2\rangle$, where α (resp. β) stands for the AA fluctuations in the x (resp. y) direction (parallel to the right ascension (resp. declination)). The brackets $\langle\rangle$ stand for temporal average. This function is zero for $\tau = 0$ and saturates to a value D_{sat} for $\tau \longrightarrow \infty$. We define its characteristic time $\tau_{\alpha|\beta}$ as the value of τ for which $D_{\alpha|\beta}(\tau_{\alpha|\beta}) = D_{\text{sat}}/e$. $\tau_{\alpha|\beta}$ is indeed the AA coherence time. The effective wind speed as well as its direction γ are derived from τ_α and τ_β using eqs. 10 and 11 of [10], taking $k' = e$. This effective wind is then, combined with the Fried parameter r_0 in the Roddier Eq. above to provide estimations of the coherence time τ_0.

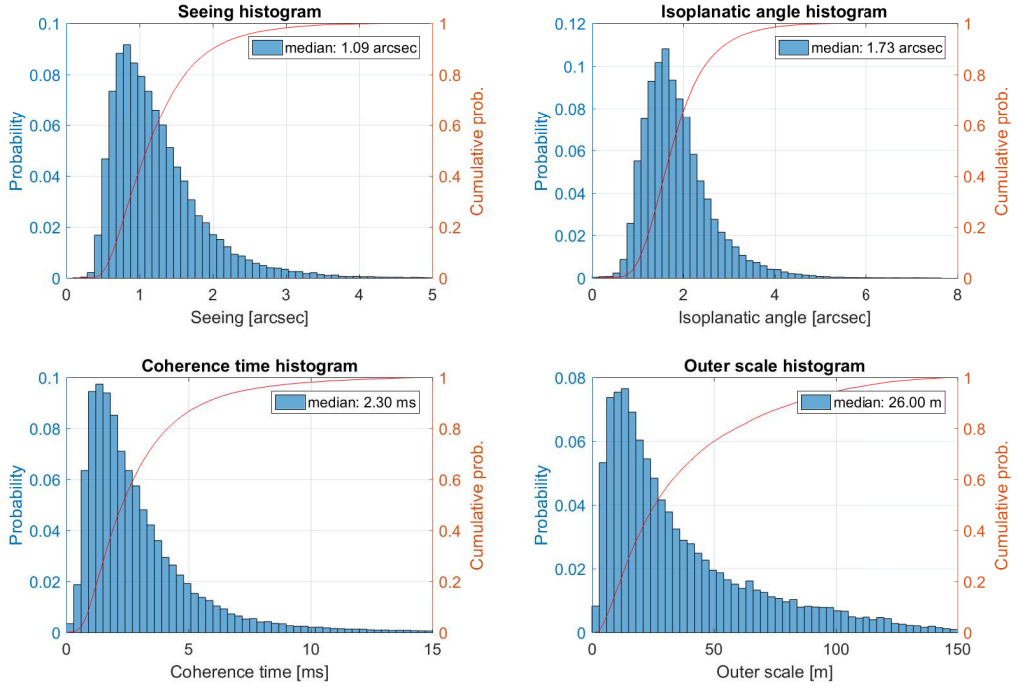

Figure 3. Histograms of turbulence parameters at Calern Observatory at $\lambda = 0.5\mu$m.

Observations with GDIMM are composed of continuous sequences of less than 1 minute of time, each sequence giving one set of turbulence parameters: seeing ϵ (two values are calculated, longitudinal ϵ_t and transverse ϵ_l), isoplanatic angle θ_0, outer scale $\mathcal{L}_0$ and coherence time τ_0. The acquisition software computes in real time all these atmospheric turbulence parameters which are sent to CATS website (Fig. 7) and displayed on the screen.

The CATS station is operational since mid-October 2015. A total of 70097 turbulence parameter measurements (22698 for $\mathcal{L}_0$) were collected at Calern observatory during the $3\frac{1}{2}$ year period from June 2015 to October 2018. Half of the data were obtained during the Summer season (June to September) where meteo conditions are better. Statistics of the 4 turbulence parameters (ϵ_0, θ_0 τ_0, $\mathcal{L}_0$) are presented in.[6] Histograms are displayed in Fig. 3 and show a classical log-normal shape for all parameters. Compared to other astronomical sites in the world (for example Paranal, La Silla and Mauna Kea are given in[6]) show that the Calern plateau is an average site.

The seeing is slightly lower in summer, we measured a median value of $0.96arcsec$ in July and August (the median winter seeing during the period November–January is $1.21arcsec$). As a consequence, the median

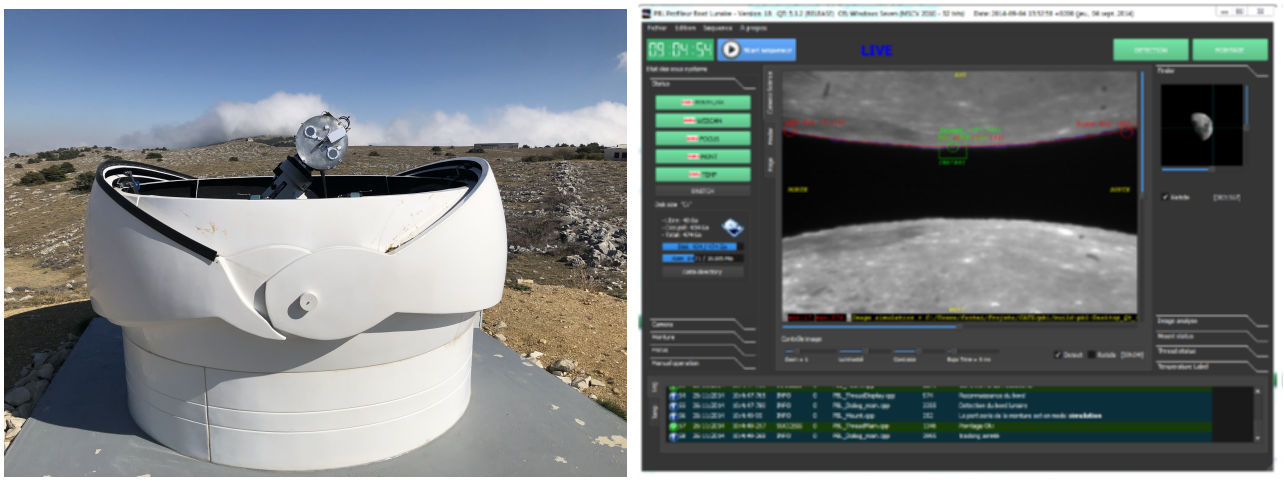

Figure 4. Left: the Profiler of Moon Limb instrument inside its 12ft AllSky dome. Right: The graphical user interface of the PML instrument showing the two Moon limb images.

coherence time is higher in summer (3.2ms in July–August, 2.40ms in November–January). The outer scale $\mathcal{L}_0$ has values similar to other sites such as Mauna Kea or La Silla.

Sequences of several hours of good seeing were sometimes observed, which is a good point for this site (and already known by "old" observers on interferometers during the 80's and 90's). Indeed, for example the median seeing for the night of 12/21/2018 was 0.64" which is an exceptional night in terms of image quality and comparable to what is obtained in the best sites over the world such as Paranal, Mauna Kea and Dome C in Antartica (Fig. 7).

2.2 The PML instrument

The PML (Profiler of Moon Limb) instrument is mainly dedicated to the extraction of the C_n^2 profile with high vertical resolution from lunar (or solar) limb fluctuations. The PML instrument is based on a differential method by observation of the lunar (or solar) limb through two sub-apertures (Fig. 4). The Moon or Solar limb acts as a continuum of double stars with all possible angular separations required between two points to scan the atmosphere with a very fine resolution.

The PML instrument consists of a 16-inch telescope (Meade M16) installed on an Astrophysics AP3600 mount. The pupil mask, composed of two sub-apertures of diameter $D = 6$cm separated by a baseline $B = 26.7$ cm, is placed at the entrance pupil of the telescope. An optical system is installed at the ouput of the telescope. It consists of a collimated beam by using a first lens L1 placed at its focal length from the telescope focus.[4] Then, two parallel beams are formed at the output of L1 corresponding to each sub-aperture. A Dove prism is inserted on one of the two beams to reverse one of two images of the lunar (solar) edge in order to avoid an overlapping of the two images of the Moon/Sun.[4] A second lens L2 is used to form the two images of the Moon limb (or Sun edge) on the CCD camera. Each optical element is placed on a micro-control plate allowing fine adjustments. To compensate for variations in the telescope's focus because of the temperature variations, we installed the CCD camera on an automatic micro-control plate controlled by the acquisition software (Fig. 4). Images at the focal plane are recorded using a PixelFly CCD camera with 640×480 pixel matrix. In order to freeze atmospheric effects on the motion of the Moon's (or Sun's) limb image and to have enough flux, the exposure time is set to 5ms.

The principle of the PML instrument is based on the measurement of the angular correlation of the fluctuation differences in the wavefront AA deduced from the motion of the Moon's (or Sun) limb image. The AA fluctuations are measured perpendicularly to the lunar (or solar) limb leading to transverse correlations for different angular separations along the Moon (or Sun). The lunar (or solar) limb is observed through two sub-apertures of diameter D= 6cm separated by a baseline B= 26.7cm when looking the edge is parallel to the baseline. In this case, the transverse covariance of the difference of the AA fluctuations (motion of the Moon or Sun limb) α between

the two images of the lunar (or solar) limb (Fig. 4) corresponds to $C_{\Delta\alpha}(\theta) = \langle[\alpha(r,\theta_0) - \alpha(r+B,\theta_0)][\alpha(r,\theta+\theta_0) - \alpha(r+B,\theta+\theta_0)]\rangle$, where $\alpha(r,\theta_0)$ and $\alpha(r,\theta+\theta_0)$ represent the fluctuations of the lunar (or solar) limb image observed through the first subaperture of the PML and measured at the angular positions θ_0 and $\theta+\theta_0$, respectively. While, $\alpha(r+B,\theta_0)$ and $\alpha(r+B,\theta+\theta_0)$ are the measured fluctuations corresponding to the second subaperture. The arbitrary angular position θ_0 is considered equal to zero. This angular covariance is a function of the spatial covariance which for the whole atmosphere is given by,

$$C_{\Delta\alpha}(\theta) = \int dh\; C_N^2(h)\; K_\alpha(B,h,\theta) \tag{3}$$

where the kernel $K_\alpha(B,h,\theta) = 2\,C_\alpha(\theta h) - C_\alpha(B-\theta h) - C_\alpha(B+\theta h)$ is a triplet of normalized spatial covariances which in the case of the von Kàrmàn model for a baseline ϱ, a sub-aperture diameter D (here 6cm), and a single layer at altitude h is given by[18]

$$C_\alpha(\varrho) = 1.19\; sec(z) \int df f^3 (f^2 + \frac{1}{\mathcal{L}_0(h)^2})^{-11/6} [J_0(2\pi f\varrho) + J_2(2\pi f\varrho)][2\frac{J_1(\pi Df)}{\pi Df}]^2 \tag{4}$$

where f is the modulus of the spatial frequency, z is the zenithal distance and $\mathcal{L}_0(h)$ is the outer scale profile.

The spatial covariance triplet above is similar to the Scidar's one.[19] The position of the lateral peak defines the altitude of the turbulent layer so that its energy is given by the peak's amplitude. For the whole atmosphere we have a superposition of different triplets corresponding to different turbulent layers.

Eq.4 is non-linear but analytical solution of the integral expression has been made by Conan et al.[20] through the use of Mellin transform. Resulting covariances are simplified into series or finite solutions. Approximations however are different depending on the baseline length. We used these approximations and the assumption of a discrete turbulent profile to transform eq.3 into $C_{\Delta\alpha}(\theta) = \sum \Delta h_i\; C_N^2(h)\; \widehat{K}_\alpha(B,h_i,\theta)$ where $\widehat{K}_\alpha(B,h_i,\theta)$ is the modified spatial covariance triplet and Δh_i is the thickness of the layer i. This equation is equivalent to a matrix form: $Y = M.X$ where X and Y are both vectors corresponding respectively to the sampled $C_N^2(h_i)$ and the covariance difference $C_{\Delta\alpha}(\theta)$, the matrix M contain the modified spatial covariance triplet weighted with Δh_i : $M = \widehat{K}_\alpha(B,h_i,\theta_j).\Delta h_i$.

The $C_N^2(h)$ profiles are retrieved by solving an inverse problem.[21,22] A full description of the algorithm will be published in a forthcoming paper. PML instrument errors are mainly related to the detection of the Moon limb position and are mostly due to photon noise.

The PML acquisition software, similar to GDIMM's one, extracts the AA fluctuations of both lunar limb (or solar edge) and save them as .csv files. The theoretical background for the computation of the $C_n^2(h)$ profile from the AA fluctuations is given in.[4] A real time computation of this profile is now integrated in the acquisition software. We are able to generate a high resolution vertical profile of C_n^2 every 2-3 minutes. The acquisition software computes in real time the $C_n^2(h)$ profile and other parameters (seeing and isoplanatic angle) which are sent to PML website as shown in Fig. 8.

In addition, the PML instrument is now equipped with automatic panels to cover the two subapertures with solar filters for a fast and automatic switch from night/Moon to day/Solar observations (Fig. 4). We then have a unique tool to study the turbulence conditions at the daytime to nightime transition as you can see in Fig. 5. Other parameters of turbulence are also accessible from this instrument such as the profile of outer scale, the seeing, and the isoplanatic and isopistonic angles.

Fig. 5 shows an example of the turbulence profile evolution with the PML throughout the daytime and the nighttime for the period of 23-25 October, 2018 at the Calern Observatory. The figure shows the full PML profiles with 33 layers from the Sun between 7am and 5pm and the rest of the time from the Moon. The resolution obtained by the PML is $\Delta h = 100m$ for the ground layer ($h \leq 1km$), $\Delta h = 500m$ for the low free atmosphere ($1km < h < 5km$), $\Delta h = 1000m$ for the mid-free atmosphere ($5km < h < 15km$), and $\Delta h = 2000m$ for the high free atmosphere ($h > 15km$). The highest altitude h_{max} reachable with the PML is more than $50km$ but we limited h_{max} to $25km$ since the turbulence is very low above this altitude. The limited field of view of the PML instrument limits the lowest measurable altitude to around $100m$. The contribution of the lowest layer

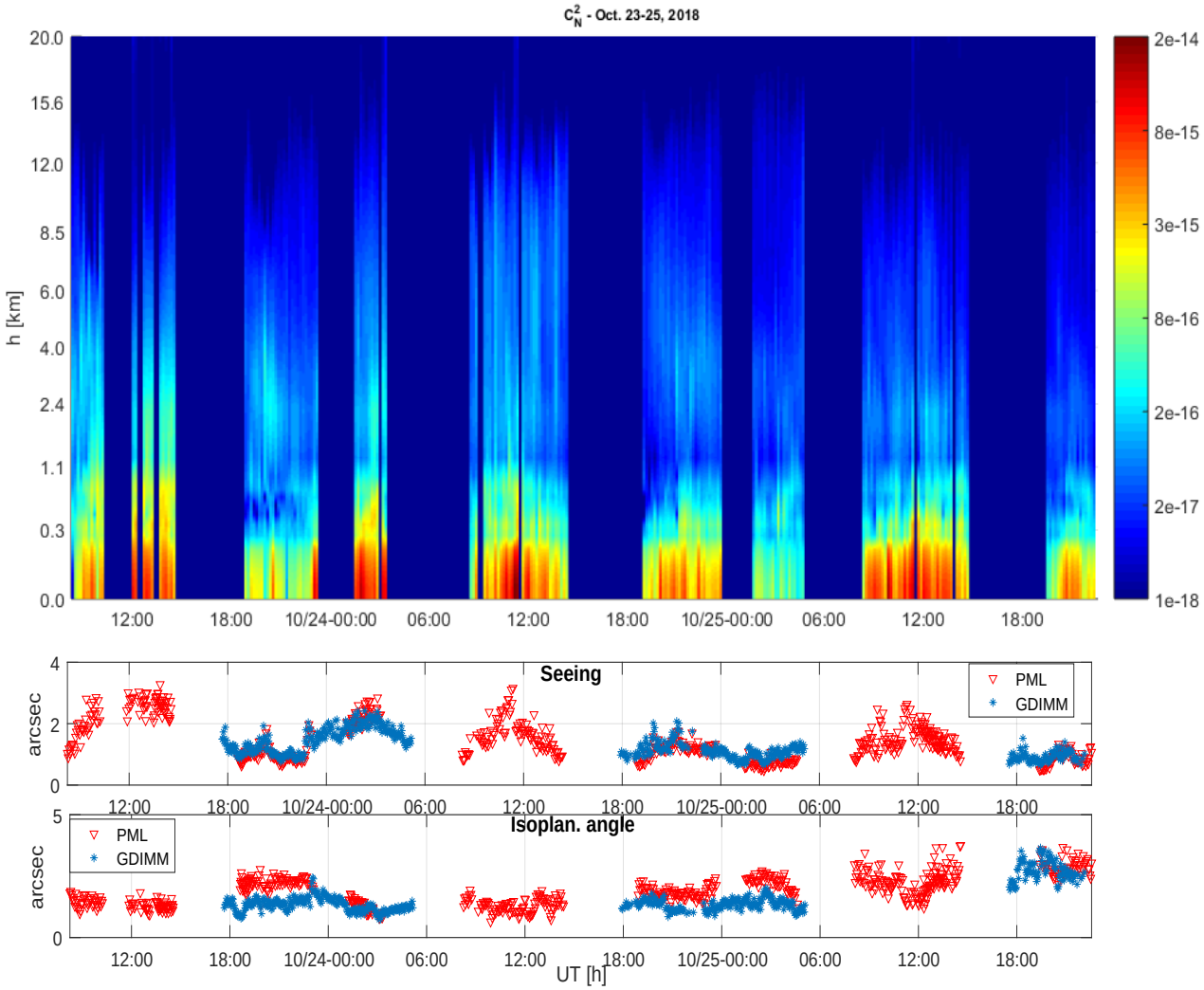

Figure 5. Turbulence C_n^2 profiles for the period of 23-25 October, 2018 obtained with the PML instrument at the Calern Observatory (Top). The altitude is given above the Calern Observatory (1270m). Observations have been obtained on the Sun edge between 7am and 5pm and on the Moon limb for the rest of the time. Bottom: Corresponding seeing and isoplanatic data obtained from the PML C_n^2 profiles above and compared with the GDIMM measurements. The isoplanatic PML results are obtained using the C_n^2 profiles when GDIMM θ_0 is deduced from scintillation.

$0 - 100m$ is obtained by the difference between the profile deduced from the inversion of the PML covariances and the total seeing from DIMM method (Sect. 2.1) using PML data. For the total seeing obtained from PML, we have about 620 estimations (each point of the Moon limb leads to a DIMM measurement) and we keep only the median one (Middle panel of Fig. 5). This PML seeing measurement is in excellent agreement with the GDIMM's data as shown in the middle panel of Fig. 5. Furthermore, the C_n^2 profiles and Fried parameters obtained with PML are used to provide the isoplanatic angle estimations as explained in.[23] These θ_0 estimations from PML instrument are presented in the bottom panel of Fig. 5. It is worth noting that isoplanatic values improve at night with respect to daytime, because the seeing conditions progressively improve when switching from Sun to Moon observations. But on average, daytime and nighttime θ_0 are comparable since it is dominated by the high layers in the atmosphere, which are similar for daytime and nighttime because they only depend on large scale meteorological phenomena. It is also interesting to point out a correlation between seeing and isoplanatism, particularly around noon, which implies that the high altitude turbulence contribution to the seeing is not negligible compared to the ground layer: Around noon is when the worst seeing conditions occur with turbulence occurring up to $20km$, as shown on the C_n^2 profiles on Fig. 5.

2.3 CATS weather conditions instrumentation

The CATS station has been designed to be autonomous without human intervention. Indeed, CATS is equipped with an AllSky camera to detect the presence of clouds in the sky and a weather station for monitoring, tem-

perature, humidity, dew point and wind velocity. All these sensors information is treated by a software devoted to observation management.

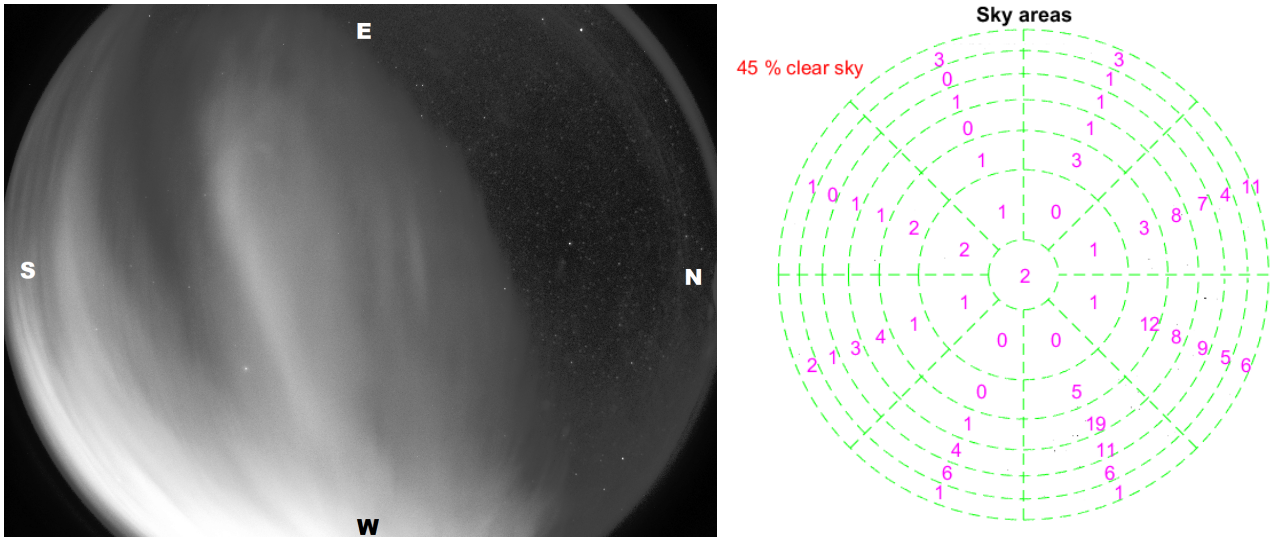

Figure 6. All-Sky raw image of a partially cloudy sky, taken on Feb 12th, 2018 at 2:49 UT (left). Cardinal points (N, S, E, W) are displayed on the picture. Right: Division of the sky into a 49 zone chart of same angular surface (276 square degrees). In each zone we printed the number of detected stars. The clear sky fraction was estimated to 45% .

2.3.1 AllSky Camera

The estimation of the clear sky fraction is derived from images given by wide angle "All-Sky" camera. We use an Oculus Starlight having a field of view of 150 degrees, equipped with a CCD of 1392x1040 pixels. An exposure time of 60s gives images of the sky up to a visual magnitude of 5 to 6, containing 700 to 1000 detectable stars when the sky is totally clear. We make an image every two minutes. Images are delivered to a PC by a USB link, and are processed in real time to provide the clear sky fraction. The data processing pipeline is the following:

- A high-pass filter (fuzzy mask) is applied to images to remove wide-scale illumination gradients due to the light pollution or moonlight scattered by the clouds. This outputs into images with constant sky background, which is then easy to remove by applying a threshold.
- Individual bad points are removed by applying a 2D median filter.
- The image is divided on a polar grid, into 8 angular sectors radiating from the zenith (center of the field of view) and 7 circular rings. The radii of these rings is calculated so that the surface of the delimited circular crowns are identical. This results into a division of the whole sky into 49 zones of 276 square degrees, up to a zenith distance of 70 (we chose to exclude the first 20 above the horizon, which we almost never use for observations).
- In each of the 49 zones, we count the number of stars. This gives the chart displayed on Fig. 6. The average number of stars per zone is between 10 and 20, depending of the location in the sky (more stars are detected in the Milky Way).
- The clear sky fraction is calculated as the number of zones containing more than two stars divided by the total zone number (49).

The chart gives a mapping of the distribution of clouds in the sky and gives access to fine monitoring of the cloud cover of each zone (Fig. 6). At present we do not use this information (we compute only the total clear sky fraction), but it can be made available for further applications.

2.3.2 Weather Station

In addition, the CATS station is also equipped with a weather station which is commercial Vantage pro 2 connected to a Banana-Pi computer. It provides all the necessary quantities (temperature, humidity, pressure, dew point, wind speed and rain gauge) for a constant monitoring.

A small software called "cats weather" has been written in python to gather all the data from the AllSky camera software (fraction of sky covered by clouds) and from the weather station. From this database, the software determines if the conditions are good enough to let the two instruments open their domes and start their observations. If the sky becomes too cloudy or if outside temperature becomes too close of the dewpoint temperature, the software forces to close both domes in order to protect instruments from rain or fog. If the wind speed is above 30 km/h, observations are stopped and domes are closed, as both instruments are shaken and no data can be acquired.

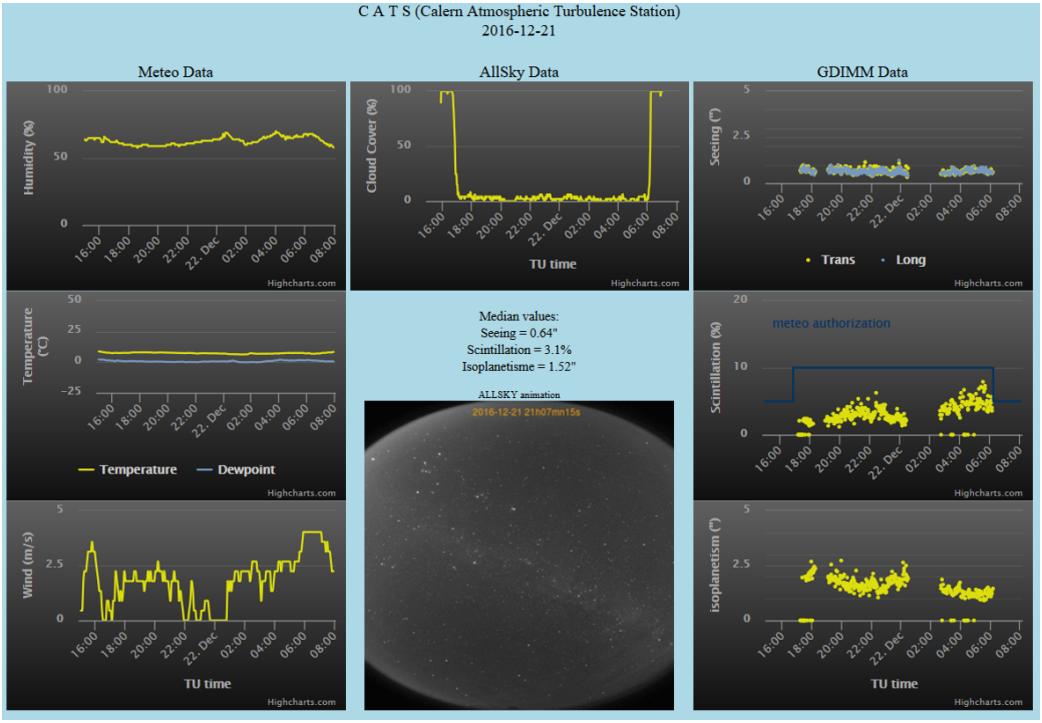

Figure 7. The GDIMM real time data website.

3. DISCUSSION

The CATS station is installed and operational at the Calern Observatory since autumn 2015. CATS is a new generation station of atmospheric turbulence measurement which is equipped with a set of complementary instruments for monitoring atmospheric turbulence parameters. The CATS station is completely autonomous without human intervention for a fully monitoring of the turbulence within original techniques since the first meters above the ground to the borders of the atmosphere. CATS station provides a real-time turbulence conditions over the Calern Observatory. The CATS station is a support involved in many scientific and educational projects at the Calern observatory such as an ongoing study of turbulence impact on the laser links of the MeO Laser Ranging Station, development of Adaptive Optics projects. Indeed, different campaigns involving optical telecommunication from space to ground with the SOTA satellite and MéO laser ranging station has already benefit of the presence of the CATS station on the Calern Plateau.[24] CATS data was jointly used with T2L2 space mission data to study laser uplink propagation in the atmosphere. The CATS station is now a routine support for observers at the satellite and lunar laser ranging station MéO. It is the very first time that a permanent instrumentation at the ground is installed next to a laser ranging station and associated with a space instrument to study the

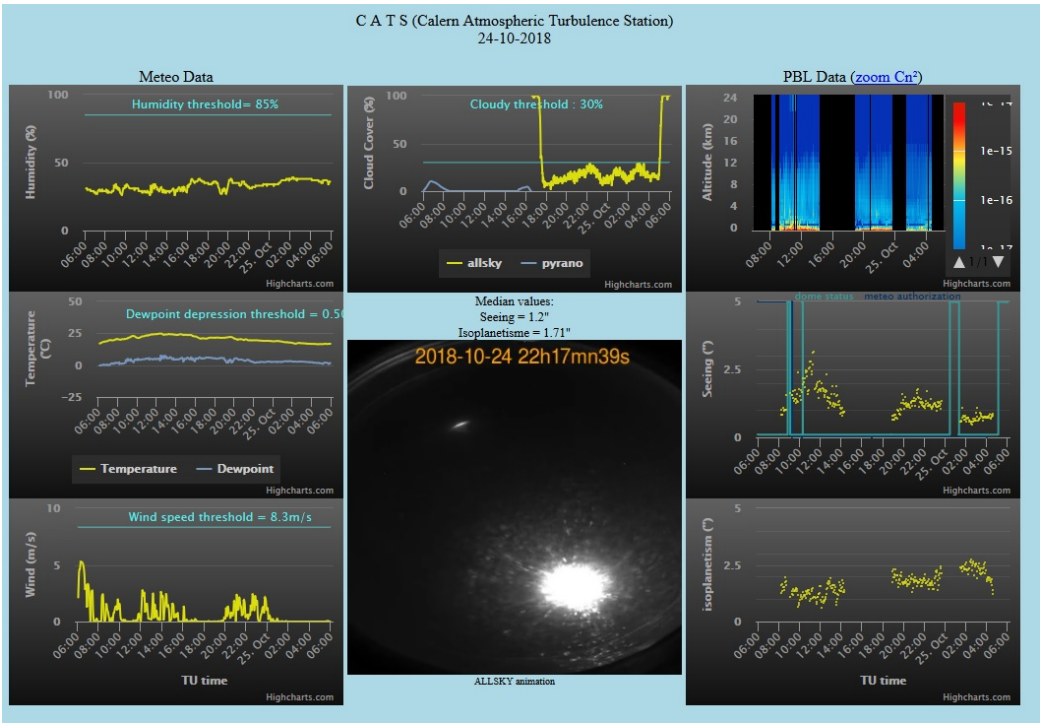

Figure 8. The PML real time data website.

turbulence effects on laser link budget from ground to space.[25] Another campaign has been performed with the Optical PAyload for Lasercomm Science (OPALS) on International Space Station in spring 2016 and recently with the DLR OSIRIS instrument. The PML instrument is very useful to understand the link budget of the lunar laser ranging activity at the MéO telescope. Several projects regarding adaptive optics systems are planned at the MéO telescope and C2PU telescope and they will benefit of the data given by the CATS station. The CATS station is also a support for another programme on the prediction of the turbulence. Data provided by CATS are used to constraint the modeling to optimize the prediction (see the publication of C. Giordano et al. in this conference). Finally, the CATS station is used for on sky practical work for students for the OPTICS master and for the international Master in Astrophysics of Université Côte d'Azur (MAUCA).

4. ACKNOWLEDGMENTS

This CATS project has been done under the financial support of CNES, Observatoire de la Côte d'Azur (OCA), Labex First TF, AS-GRAM, Federation Doblin, Université de Nice-Sophia Antipolis and Region Provence Alpes Côte d'Azur. We would like to thank all the technical and administrative staff of the Observatoire de la Côte d'Azur, our mechanical engineer Christophe Bailet and our colleagues from the AstroGéo team from GéoAzur laboratory for their help and support all along the project namely Pierre Exertier, Etienne Samain, Dominique Albanèse, Mourad Aimar, Jean-Marie Torre, Emmanuel Tric, Thomas Lebourg and Sandrine Bertetic. We thank also Christophe Giordano for his careful reading of this paper.

REFERENCES

[1] Chabé, J., Ziad, A., Aristidi, E., Fanteï-Caujolle, Y., Renaud, C., Blary, F., and Marjani, M., "The calern atmospheric turbulence station," *Astronomical Telescopes+ Instrumentation, Proc. SPIE 9906, 99064Z* (2016).

[2] Ziad, A., Chabé, J., Fanteï-Caujolle, Y., Aristidi, E., and Renaud, C., "Cats: a new station for a complete characterization of atmospheric turbulence," *Proc. AO4ELT5* (2017).

[3] Ziad, A., Chabé, J., Fanteï-Caujolle, Y., Aristidi, E., Renaud, C., and Ben Rahhal, M., "Cats: an autonomous station for atmospheric turbulence characterization," *Proc. of the SPIE 10703, 107036L* (2017).
[4] Ziad, A., Blary, F., Borgnino, J., Fantei-Caujolle, Y., Aristidi, E., Martin, F., Lanteri, H., Douet, R., Bondoux, E., and Merkarnia, D., "First results of the pml monitor of atmospheric turbulence profile with high vertical resolution," *A&A* **559**, L6 (2013).
[5] Aristidi, E., Fanteï-Caujolle, Y., Ziad, A., C., D., Chabé, J., and Roland, B., "A new generalized differential image motion monitor," *Astronomical Telescopes+ Instrumentation, Proc. SPIE 9145, 91453G* (2014).
[6] Aristidi, E., Ziad, A., Chabé, J., Fanteï-Caujolle, Y., Renaud, C., and Giordano, C. *Monthly Notices of the Royal Astronomical Society* **486**, 915 (2019).
[7] Chabé, J., Blary, F., Ziad, A., Borgnino, J., Fantei-Caujolle, Y., Liotard, A., and Falzon, F., "Optical turbulence in confined media : part i, the indoor turbulence sensor instrument," *Applied Optics* **55**, 7068 (2016).
[8] Blary, F., Chabé, J., Ziad, A., Borgnino, J., Fantei-Caujolle, Y., Liotard, A., and Falzon, F., "Optical turbulence in confined media : part ii, first results using the intense instrument," *Applied Optics* **56**, 6272 (2017).
[9] Ziad, A., Conan, R., Tokovinin, A., Martin, F., and Borgnino, J. *Applied Optics* **39**, 5415 (2000).
[10] Ziad, A., Borgnino, J., Ali, W. D., Berdja, A., Maire, J., and Martin, F., "Temporal characterization of atmospheric turbulence with the generalized seeing monitor instrument," *Journal of Optics* **14**(4), 045705 (2012).
[11] Sarazin, M. and Roddier, F., "The eso differential image motion monitor," *Astronomy and Astrophysics, vol. 227, no. 1, Jan. 1990, p. 294-300.* (1990).
[12] Aristidi, E., Agabi, A., Fossat, E., Azouit, M., Martin, F., Sadibekova, T., Travouillon, T., Vernin, J., and Ziad, A., "Site testing in summer at dome c, antarctica," *A&A* **444**(2), 651–659 (2005).
[13] Loos, G. and Hogge, C., "Turbulence of the upper atmosphere and isoplanatism," *Applied Optics* **18**, 15 (1979).
[14] Ziad, A., "Review of the outer scale of the atmospheric turbulence," *Astronomical Telescopes+ Instrumentation, Proc. SPIE 9909, 99091K, Invited Speaker* (2016).
[15] Ziad, A., Borgnino, J., Martin, F., and Agabi, A., "Experimental estimation of the spatial-coherence outer scale from a wavefront statistical analysis," *A&A* **282**, 1021–1033 (feb 1994).
[16] Aristidi, E., Fanteï-Caujolle, Y., Chabé, J. A., C., R., Ziad, and Ben Rahhal, M., "Turbulence monitoring at the plateau de calern with the gdimm instrument," *Astronomical Telescopes+ Instrumentation, Proc. SPIE (this conf.)* (2018).
[17] Roddier, F., Gilli, J., and Lund, G. *J. Opt. (Paris)* **13**, 263 (1982).
[18] Avila, R., Ziad, A., Borgnino, J., Martin, F., Agabi, A., and Tokovinin, A., "Theoretical spatiotemporal analysis of angle of arrival induced by atmospheric turbulence as observed with the grating scale monitor experiment," *J. Opt. Soc. Am. A* **14**, 3070–3082 (Nov 1997).
[19] Fuchs, A., Tallon, M., and Vernin, J. *PASP* **110**, 86 (1998).
[20] Conan, R., Borgnino, J., Ziad, A., and Martin, F. *J. Opt. Soc. Am.* **17(10)**, 1807 (2000).
[21] Blary, F., *Caractérisation et Modélisation de la Turbulence Optique dans un espace confiné*, PhD thesis, Université de Nice Sophia Antipolis (2015).
[22] Catala, L., Ziad, A., Fanteï-Caujolle, Y., Crawford, S. M., Buckley, D. A. H., Borgnino, J., Blary, F., Nickola, M., and Pickering, T. *Monthly Notices of the Royal Astronomical Society* **467**, 3699 (2017).
[23] Ziad, A., Aristidi, E., Chabé, J., and Borgnino, J. *Monthly Notices of the Royal Astronomical Society* **487**, 3664 (2019).
[24] Vedrenne, N., Velluet, M.-T., Petit, C., Michau, V., Phung, D.-H., Maurice, N., Samain, E., Chabé, J., Ziad, A., Artaud, G., Issler, J.-L., Toyoshima, M., Akioka, M., Kolev, D. R., Munemasa, Y., Takenaka, H., and Iwakiri, N., "First results of wavefront sensing on SOTA," in [*2015 IEEE International Conference on Space Optical Systems and Applications (ICSOS2015)*], (Oct. 2015).
[25] Sinclair, L. C., Giorgetta, F. R., Swann, W. C., Baumann, E., Coddington, I., and Newbury, N. R., "Optical phase noise from atmospheric fluctuations and its impact on optical time-frequency transfer," *Phys. Rev. A* **89**, 023805 (Feb 2014).